

phys. stat. sol. (a) **121**, 483 (1990)

Subject classification: 64.75; 61.55; S1.1

Ottawa-Carleton Institute for Physics, University of Ottawa¹⁾ (a) and
Centro de Estudios de Semiconductores, Departamento de Física, Facultad de Ciencias,
Universidad de Los Andes, Merida²⁾ (b)

$T(z)$ Diagram of $\text{CuIn}_{1-z}\text{Fe}_z\text{S}_2$ Alloys

By

R. BRUN DEL RE (a), J. C. Woolley (a), M. QUINTERO (b), and R. TOVAR (b)

The $T(z)$ phase diagram of the system $\text{CuIn}_{1-z}\text{Fe}_z\text{S}_2$ is obtained from differential thermal analysis and X-ray diffraction measurements. It is found that the range of solid solution in the terminal chalcopyrite compounds at 200 °C is limited to $0 < z < \approx 0.20$ for the CuInS_2 α -phase and $\approx 0.94 < z < 1.0$ for the CuFeS_2 γ -phase. At higher temperatures, the cubic zinc-blende β -phase is found to extend across practically the whole composition range. Samples with $0.2 < z < 0.6$, when rapidly quenched from the β field, show a metastable α -chalcopyrite condition, giving a useful extension of the composition range of the α -structure. At high values of z , the form of the diagram is complicated at higher temperatures by the dissociation of CuFeS_2 into a zinc-blende phase β' and pyrite.

Aus Differentialthermoanalyse und Röntgenbeugungsmessungen wird das $T(z)$ -Phasendiagramm des Systems $\text{CuIn}_{1-z}\text{Fe}_z\text{S}_2$ erhalten. Es wird gefunden, daß der Bereich der festen Lösung in den Chalkopyrit-Endverbindungen bei 200 °C auf $0 < z < \approx 0,20$ für die CuInS_2 - α -Phase und auf $\approx 0,94 < z < 1,0$ für die CuFeS_2 - γ -Phase begrenzt ist. Es wird gefunden, daß sich die kubische Zinkblende- β -Phase bei höheren Temperaturen praktisch über den gesamten Zusammensetzungsbereich erstreckt. Bei schnellem Abschrecken vom β -Feld, zeigen Proben mit $0,2 < z < 0,6$ einen metastabilen α -Chalkopyritzustand und ergeben eine nützliche Erweiterung des Zusammensetzungsbereichs der α -Struktur. Bei hohen Werten von z ist die Form des Diagramms bei höheren Temperaturen infolge der Dissoziation von CuFeS_2 in eine Zinkblendenphase β' und Pyrit komplizierter.

1. Introduction

The large majority of works published on semimagnetic semiconductors is concerned with alloys involving manganese, mostly derived from II–VI compounds [1, 2]. Recently, alloys based on chalcopyrite I–III–VI₂, with Mn atoms replacing equal numbers of I and III atoms, have been studied (e.g. [3, 4]). However, alloys involving other magnetic elements have received very little attention. In the case of iron, one obvious possibility is again alloys involving I–III–VI₂ compounds since some I–Fe–VI₂ compounds show the chalcopyrite structure. Only a few cases of these alloys have been discussed in the literature. Teranishi et al. [5] investigated the magnetic properties of the $\text{CuAl}_{1-z}\text{Fe}_z\text{S}_2$ alloys and their results show that the solid solution in the CuAlS_2 phase extends to at least $z = 0.16$. The $\text{CuGa}_{1-z}\text{Fe}_z\text{S}_2$ alloys were studied by Digiuseppe et al. [6] and in this system there is a single phase solid solution across the complete composition range. Finally, Wasim et al. [7] have done some work on the $\text{CuIn}_{1-z}\text{Fe}_z\text{Te}_2$ alloys and indicate a range of solid solutions up to $z = 0.3$. In the present, work the alloy system $\text{CuIn}_{1-z}\text{Fe}_z\text{S}_2$ is investigated.

¹⁾ 34 George Glinski, Ottawa, Ontario, K1N 6N5, Canada.

²⁾ Merida, Venezuela.

2. Preparation of Alloys and Experimental Measurements

The alloys were produced by melting together the appropriate weights of the constituent elements. The components of each 1 gm sample were sealed under vacuum in a quartz capsule and melted together at 1150 °C. The resulting alloy was then slowly cooled in the furnace, taking about three days to reach room temperature. When details of the $T(z)$ diagram had been obtained, samples were annealed to equilibrium at various temperatures for X-ray analysis of the equilibrium condition, and also for magnetic and Mössbauer measurements. Details of these heat treatments are given below.

Standard closed-tube differential thermal analysis (DTA) measurements [8] were made in the temperature range from room temperature to 1100 °C with silver used as the reference material. The charge was powdered alloy of approximately 100 mg weight. This was sealed under vacuum in a small quartz ampoule which had a re-entrant thermocouple well at the bottom. The temperatures of the sample and the reference were measured with chromel–alumel thermocouples, the difference signal between sample and reference and the temperature signal being recorded. Each phase transition temperature was determined from the base-line intercept of the tangent to the leading edge of the peak in the difference signal. Both heating and cooling runs were made for each sample.

3. Results and Discussion

Samples were prepared to cover the complete composition range in steps of 0.1 in z with extra compositions being added at the two ends of the composition range. DTA measurements were made on all of the samples and values of the various transition temperatures for each sample were determined. The resulting $T(z)$ diagram is shown in Fig. 1, where boundaries from the DTA data are shown as full lines, with dashed lines being used to indicate estimated boundaries.

For CuInS_2 (i.e. $z = 0$), transitions were observed at the temperatures 935, 1020, and 1052 °C. These transitions correspond to those reported by Binsma et al. [9] and attributed, respectively, to the transitions chalcopyrite α to zincblende β , β to an undetermined phase

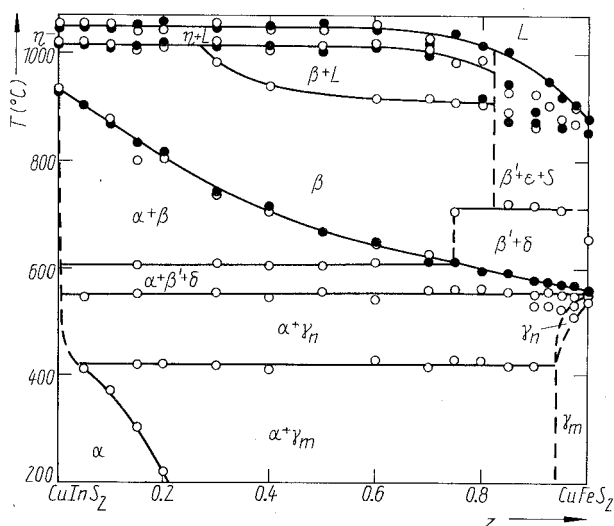


Fig. 1. $T(z)$ diagram for the $\text{CuIn}_{1-z}\text{Fe}_z\text{S}_2$ alloy system. \circ DTA heating run, \bullet DTA cooling run. — phase boundaries from DTA data, - - - estimated boundaries. α CuInS_2 chalcopyrite, γ_m magnetic CuFeS_2 chalcopyrite, γ_n non-magnetic CuFeS_2 chalcopyrite, β and β' phases with zincblende structure, δ pyrite FeS_2 , ϵ pyrrhotite $\text{Fe}_{1-\delta}\text{S}$, S sulphur, η phase of unknown structure (possibly wurtzite)

η (possibly wurtzite), and η to liquid. For CuFeS_2 (i.e. $z = 1.0$), the behaviour is more complex, involving the complicated behaviour of the Cu–Fe–S diagram. Previous work [10] indicates that the compound CuFeS_2 is antiferromagnetic with a Néel temperature of 550°C . At a slightly higher temperature of 557°C , a transition occurs [11] which is not merely an inversion to a less ordered phase, but decomposition to a face-centred cubic phase, very similar to the zincblende β phase and labelled here β' , plus pyrite FeS_2 , labelled here δ . The isothermal section of the Cu–Fe–S diagram at 600°C (12) would indicate a molecular ratio of approximately twelve parts of β' phase to one of pyrite for stoichiometric CuFeS_2 . According to Kullerud and Yoder [13], pyrite is stable to 743°C where it undergoes a peritectic breakdown to pyrrotite and sulphur, labelled in Fig. 1 as ϵ and S, respectively. This would produce a further transition peak to be observed for CuFeS_2 . In the present work, transition peaks were obtained consistent with the above results. In addition, two transitions were observed at higher temperatures, the higher one at 930°C being taken as the liquidus point for the β' phase.

From the consideration of this known behaviour of the terminal compounds and from an analysis of X-ray photographs of alloys annealed under appropriate conditions, the various alloy fields were labelled as shown in Fig. 1. It is seen that the range of solid solubility in the α phase is very small at temperatures above 450°C but increases appreciably at lower temperatures, being 0.21 at 200°C . Samples in the range $0 < z < 0.4$ were annealed at 200°C for three weeks to give equilibrium conditions and X-ray powder photographs were taken of each. The resulting values of the lattice parameter a are shown in Fig. 2. These data indicate a limit of single phase behaviour at $z = 0.19$, in reasonable agreement with the DTA data. In these alloys, the value of c/a was found to vary practically linearly from 2.02 at $z = 0$ to 2.00 at the limit of single phase behaviour.

Outside the α field, the $T(z)$ diagram can be considered in two parts separated by the transition at 550°C , which corresponds to the decomposition of the γ phase described above, and which extends across the complete composition range. At lower temperatures, over a wide composition range, the equilibrium condition is two phase, $\alpha + \gamma$. However, a transition is observed for most compositions at 420°C , which has been shown from Mössbauer measurements [14] to correspond to the Néel temperature of the equilibrium γ phase. In Fig. 1, the magnetic and non-magnetic γ phases have been labelled γ_m and γ_n , respectively.

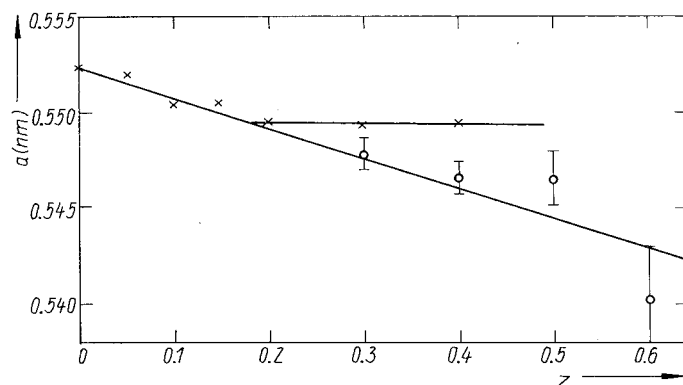


Fig. 2. Variation of lattice parameter a of the CuInS_2 chalcopyrite α phase with composition z . \times samples annealed to equilibrium at 200°C , \circ samples quenched to room temperature from 850°C

At the CuFeS_2 end of the diagram, the range of single phase behaviour in the γ phase is fairly small. The phase boundary was not detected in the DTA measurements, indicating that the boundary is a steep one, and the observed variation of the lattice parameter a in the composition range $0.85 < z < 1.0$ for samples annealed at 450°C was within the experimental scatter, so that a reasonable estimate of the field limit could not be obtained from these data. However, faint lines corresponding to the α phase could be observed for the samples with $z = 0.85$ and 0.90 . An attempt was made to determine this limit by annealing samples with $0.3 < z < 0.7$ at 200°C , determining the relative intensities of the lines of the α and γ phases in X-ray powder photographs, and then using the lever rule to find the boundaries of the two phase field. This analysis indicated boundaries at values of z of 0.21 ± 0.03 and 0.90 ± 0.08 . Similar calculations for a sample with $z = 0.85$ annealed at 200°C , assuming the limit of the α field to be 0.20 in this case, gave a value of $z = 0.94$ for the limit of the γ field. However, one complication with the alloys in the range $0.8 < z < 1.0$ was that even after long annealing at either 450 or 200°C , very faint lines of pyrite FeS_2 could be observed on the X-ray powder photographs, while peaks corresponding to FeS_2 could clearly be seen in the Mössbauer spectra of these samples [14]. From estimates of the relative intensities of the lines in the X-ray photographs, there appeared to be about 2 mol% of FeS_2 in these samples. The presence of FeS_2 is due to the form of $T(z)$ at higher temperatures, which is discussed further below. The scatter of the points in the DTA data for $0.9 < z < 1.0$ may be partially due to the presence of these small amounts FeS_2 in the samples. However, in the temperature range 450 to 550°C , the composition of the γ phase present in the two phase samples varies very rapidly with temperature, as does the Néel temperature, so that the experimental scatter of the DTA points could well be due to the samples not retaining equilibrium conditions in this range during the DTA runs. Taking the single phase limit as $z = 0.94$ and the Néel temperature at this composition as 420°C , the boundaries of the γ_m and γ_n fields have been estimated as shown in Fig. 1.

In the section of the diagram that lies above 550°C , again the fields have been labelled by comparison with the known conditions for the two terminal compounds. Thus one large single phase field exists, labelled β . This would appear to extend across the complete composition range except for the effects of the decomposition of CuFeS_2 at 557°C . Thus at values of z greater than about 0.75 , small amounts of the δ phase and at higher temperatures the ϵ and S phases are present. In this range, the zincblende-like phase has been labelled β' , since it is not known whether the $\beta(\beta')$ phase varies continuously in composition across the whole diagram, or whether there is a discontinuous change in composition at a point where the δ and ϵ phases appear, as indicated by the dashed line in the figure.

In an attempt to confirm that β was indeed a zincblende structure, samples in the range $0.2 < z < 0.7$ were annealed at 850°C and quenched in brine to try to retain the high temperature structure. However, X-ray photographs of these samples indicated that only one phase was observed, showing blurred lines, which had the chalcopyrite α structure. The photographs were very different from those for the alloys annealed at 200°C . Measurements of the lattice parameter values for the α phase in these quenched samples gave values of a shown in Fig. 2, where the error bar on the points represents the degree of blurring of the lines in the photographs. It is seen that within the accuracy of the measurements, these quenched points lie on an extension of the line obtained from the points representing the equilibrium condition at 200°C . Thus it is seen that the quenched samples are in a metastable chalcopyrite form, even though in the composition range $z > 0.2$

no stable form of this structure occurs. These results are confirmed by the magnetic susceptibility measurements [15], in which the quenched samples again showed values of the magnetic transition temperature T_0 and the Curie-Weiss temperature θ which are an extension of the values obtained in the equilibrium range of lower z . The occurrence of a metastable chalcopyrite phase in quenched samples for a composition range where the equilibrium condition is two phase, has also been observed in the $(\text{CuGa})_{1-z}\text{Mn}_z\text{Te}_2$ alloys [16]. It appears that when the samples are quenched from a cubic single phase field at higher temperatures, the diffusion rates at the lower temperatures are too low to allow the long-range diffusion needed to give the equilibrium two phase condition to take place, but the short-range diffusion to allow ordering from zinblende to chalcopyrite can occur, resulting in the metastable form observed.

As indicated above, for $z > 0.75$ the diagram is complicated by the decomposition of what would have been the β phase at CuFeS_2 , which introduces a small amount of pyrite (δ) or at higher temperatures pyrrhotite (ϵ) and sulphur (S). In the present measurements a transition was observed at 715 °C as shown in Fig. 1 which has been taken as the temperature for the transition of δ to ϵ and S, i.e. the transition from a two phase $\beta' + \delta$ field to a three phase $\beta' + \epsilon + \text{S}$ field. Because of the complicated form, no attempt has been made to label fields at higher temperatures in this composition range.

At lower temperatures, the β field is bounded by a two phase $\alpha + \beta$ field, and between that field and that of $\alpha + \gamma_n$ there is a three phase field, $\alpha + \beta' + \delta$. Above the β field, there are two two-phase fields which have been taken to be $\beta + \text{L}$ and $\eta + \text{L}$. The presence of liquid as a phase in the $\beta + \text{L}$ field was confirmed by heating samples with $z = 0.5$ and 0.6 to 950 °C. Inspection of the quenched samples then showed rounding of previously sharp edges due to melting.

4. Conclusions

The present investigation shows that the range of solid solubility in the terminal compounds is quite limited on both sides. However, for CuInS_2 the limit of the single phase field varies appreciably with temperature from $z \approx 0.02$ at 450 °C to $z \approx 0.21$ at 200 °C. For CuFeS_2 the limit of single phase behaviour is approximately $z \approx 0.94$ at all temperatures in the range 200 to 500 °C. In this single phase field, the value of the Néel temperature was found to fall from 540 °C at $z = 1$ to 420 °C at the limit of the field. At higher temperature, the zinblende phase β extends across practically the whole composition range, but for $z > 0.75$ a small amount of pyrite δ (or at slightly higher temperatures, pyrrhotite ϵ and sulphur S) occurs due to the decomposition previously observed in CuFeS_2 [11]. Samples rapidly quenched from this β field to room temperature were found to show an effectively single phase condition corresponding to the chalcopyrite α phase. This metastable phase was found from X-ray, magnetic [15], and Mössbauer [14] measurements to extend the range of the chalcopyrite α behaviour.

For $z > \approx 0.80$, samples annealed for several weeks at temperatures in the range 200 to 450 °C were found still to show traces of pyrite FeS_2 (δ) produced by decomposition of the γ_n phase at higher temperatures.

In the $\alpha + \gamma_m$, $\alpha + \gamma_n$, and $\alpha + \beta$ two phase fields, the results indicate that the tie lines lie in the plane of the plane of the diagram. However, the presence of pyrite δ , pyrrhotite ϵ , and sulphur S, due to the CuFeS_2 decomposition, means that the complete diagram does not show pseudobinary behaviour.

Acknowledgements

The authors would like to thank Dr. G. Lamarche, Dr. D. Rancourt, and M. Royer of the University of Ottawa for useful discussions. The Venezuelan authors wish to acknowledge the financial support of CONICIT and CDCHT-ULA, Venezuela.

References

- [1] J. K. FURDYNA and J. KOSSUT, Diluted magn. Semicond., Semimetals Semicond. (Ed. Willardson and Beer, Academic Press) **25**, (1989).
- [2] J. K. FURDYNA, J. appl. Phys. **64**, R29 (1989).
- [3] M. QUINTERO, P. GRIMA, R. TOVAR, G. S. PÉREZ, and J. C. WOOLLEY, phys. stat. sol. (a) **107**, 205 (1988).
- [4] C. NEAL, J. C. WOOLLEY, R. TOVAR, and M. QUINTERO, J. Phys. D **22**, 1347 (1989).
- [5] T. TERANISHI, K. SATO, and Y. SAITO, Inst. Phys. Conf. Ser. No. 35, 59 (1977).
- [6] M. DIGIUSEPPE, J. STEGER, A. WOLD, and K. KOSTINER, Inorg. Chem. **13**, 1828 (1974).
- [7] S. M. WASIM, M. ALI, N. AVGERINOS, I. S. AL-SAFFAR, and R. D. TOMLINSON, Nuovo Cimenti **D2**, 1695 (1983).
- [8] R. CHEN and Y. KIRSH, Internat. Ser. Sci. Solid State **15**, 97 (1981).
- [9] J. J. M. BINSMA, J. L. GILING, and J. BLOOM, J. Cryst. Growth **50**, 429 (1980).
- [10] T. TERANISHI, K. SATO, and K. KONDO, J. Phys. Soc. Japan **36**, 1618 (1974).
- [11] J. R. CRAIG and S. D. SCOTT, Sulphide Mineralogy, Ed. P. H. RIBBE, Mineralog. Soc. Amer., 1976 (p. CS73).
- [12] J. L. CABRI, Econ. Geol. **68**, 443 (1973).
- [13] G. KULLERUD and H. S. YODER, Econ. Geol. **54**, 533 (1959).
- [14] M. ROYER, R. BRUN DEL RE, P. HARGREAVES, and D. RANCOURT, to be published.
- [15] G. LAMARCHE, R. BRUN DEL RE, and J. C. WOOLLEY, to be published.
- [16] M. QUINTERO, P. GRIMA, R. TOVAR, R. GOUDREAU, D. BISSONNETTE, G. LAMARCHE, and J. C. WOOLLEY, J. Solid State Chem. **76**, 210 (1988).

(Received June 28, 1990)